Nuclear Physics **A504** (1989) 300–322
North-Holland, Amsterdam

METASTABLE HOT NUCLEI IN A SEMICLASSICAL DESCRIPTION*

Alex H. BLIN[1] and Matthias BRACK

Theoretische Physik, Universität Regensburg, D-8400 Regensburg, Fed. Rep. Germany

Received 25 July 1988
(Revised 6 March 1989)

Abstract: Starting from a variational equation for the grand canonical potential, the density profiles of metastable hot nuclei are calculated; the boundary conditions correspond to zero external pressure. The solutions are compared to the case of a nucleus embedded in a gas at finite pressure. The evaporation of neutrons from the hot nuclei is investigated; the evaporation lifetimes are smaller in the metastable case, where no external pressure acts on the nucleus. The Coulomb energy is found to play a dominant role; it lowers considerably the maximum temperature up to which solutions exist. The influence of the temperature on the nuclear compressibility is discussed.

1. Introduction

The existence of highly excited "hot" nuclei, even up to phase transition temperatures, has been conjectured by the experimental investigations of e.g. the Purdue group [1]). A theoretical description of hot nuclei in the framework of the temperature-dependent Hartree-Fock (HF) approximation was presented in refs. [2,3]). In ref. [4]) a semiclassical approach was used. The phase transition aspect of hot nuclei was treated semiclassically in ref. [5]) and will not be considered in this work.

In both the HF and semiclassical studies of refs. [2–4]), the nucleus is thought to be surrounded by a gas of nucleons, which provides the necessary external pressure to equilibrize the hot nucleus. In reality, this gas does not exist. Although the hot nucleus evaporates nucleons which exert a certain pressure on the nuclear surface due to momentum conservation, this pressure is far below an equilibrium situation. There are no nucleons entering the nucleus from the outside, as in the case of a nucleus in equilibrium with some external gas. We therefore adopt the opposite point of view by requiring zero outside pressure and discuss the boundary conditions which allow to find solutions in this case, although a free hot nucleus is thermodynamically unstable.

In the next section we derive the differential equations which describe the nucleus in a semiclassical approach. The cases of zero external pressure and of an external

* Supported by Deutsche Forschungsgemeinschaft, contract Br733/4, and by Hahn-Meitner-Institut, Berlin, FE-Vertrag 180/531/047572.

[1] Present address: Centro de Física Teórica do INIC, Universidade de Coimbra, P-3000 Coimbra, Portugal.

gas are presented. Then, in sect. 3, we discuss the nuclear compressibility and the giant monopole and quadrupole resonance energies of hot nuclei. Sect. 4 presents the expressions for the entropy and for the neutron evaporation times. The results of our calculations for uncharged lead are studied in sect. 5, whereas sect. 6 deals with charged ^{208}Pb. Concluding remarks are given in sect. 7. Calculational details are shown in several appendices.

2. Variational equations for the nuclear densities

We consider the hot nucleus as a grand canonical ensemble at temperature T (measured in units of MeV, putting the Boltzmann constant $k=1$). The density profiles $\rho_n(\boldsymbol{r})$ and $\rho_p(\boldsymbol{r})$ of the (spherical) nucleus are then obtained from a variational principle for the grand canonical potential Ω.

$$\frac{\delta}{\delta\rho_q}\Omega=\frac{\delta}{\delta\rho_q}\int \mathrm{d}^3r(\mathscr{F}[\rho_n(\boldsymbol{r}),\rho_p(\boldsymbol{r})]+P_0-\lambda_n\rho_n(\boldsymbol{r})-\lambda_p\rho_p(\boldsymbol{r}))=0\,, \tag{2.1}$$

with $q=n$ for neutrons, $q=p$ for protons. Here, $\mathscr{F}[\rho_n(\boldsymbol{r}),\rho_p(\boldsymbol{r})]$ is the free-energy density, P_0 the external pressure, and λ_n and λ_p are the chemical potentials for neutrons and protons.

Concerning the choice of the constant P_0, we shall discuss two different situations: (i) the case of a metastable, isolated nucleus with $P_0=0$, and (ii) the "equilibrium situation", in which the hot nucleus is assumed to be surrounded by a gas of nucleons which exerts the necessary external pressure to maintain a thermodynamical equilibrium [3]; $P_0>0$ is then the gas pressure. We shall come back to this case in sect. 2.2 below.

In the present work, we want to take a different point of view [6]. An isolated hot compound nucleus, such as one formed in a heavy-ion collision, is known not to be stable but to evaporate nucleons, i.e. the external pressure P_0 is zero. For not too high temperatures – the limits will be discussed in details below – the evaporation lifetimes are long enough so that the nucleus can be considered to be in a metastable state, very much like a superheated liquid drop (see, e.g. ref. [7]). But in order to describe this metastable system by a static variational procedure, we have to impose suitable boundary conditions.

The case of symmetric ($\rho_n=\rho_p=\frac{1}{2}\rho$), semi-infinite nuclear matter in the metastable situation has been studied in detail by Stocker and Burzlaff [8]. The free variation of the density profile $\rho(z)$ (where z is the axis perpendicular to the infinite, flat surface) *with the boundary condition* $P_0=0$ was shown there to lead to a minimum of $\rho(z)$ in the outer surface at a point z_0: $\rho'(z_0)=0$ with $\rho(z_0)=\rho_g>0$ for $T>0$. The physical interpretation given to this solution in ref. [8]) is the following. The portion of $\rho(z)$ for $z\leqslant z_0$ represents the density profile of infinite nuclear matter. The limiting density ρ_0 far inside the nucleus ($z\to\infty$) is that of nuclear matter at zero pressure and becomes equal to the saturation density at $T=0$. The density ρ_g

at $z = z_0$ is the second solution of the equation $\mathcal{F}_\infty(\rho) = \lambda\rho$, where $\mathcal{F}_\infty(\rho)$ is the volume part of the free-energy density and λ the chemical potential. The maximum temperature T_m for which solutions can be found is the so-called "flash temperature" (see also ref. [9])); at this temperature ρ_0 becomes equal to ρ_g. The temperature T_m is typically about 3 MeV lower than the critical temperature T_c for the liquid-gas phase transition in the equilibrium situation. For the SkM* force, for instance, we have $T_m = 11.6$ MeV and $T_c = 14.6$ MeV [ref. [10])]. Both these temperatures will be lowered for finite nuclei by surface, asymmetry and, especially, Coulomb effects.

In the following, we shall extend these studies [8]) to realistic, finite nuclei using the same boundary condition, i.e. $P_0 = 0$. Note that P_0 is the *external* pressure; $P_0 = 0$ does not exclude the fact that in a finite nucleus there will be a finite intrinsic pressure coming from the surface tension and from the finite compressibility of the system. Note also, that the local intrinsic pressure P_g at the surface position, $P(z_0) = P_g$, is not zero; it corresponds to the fact that the system wants to evaporate nucleons. This is in contrast to the equilibrium situation, where the pressure outside the surface, where the density has become flat, is exactly balanced by that of the assumed surrounding gas; this pressure is then the non-zero external pressure P_0, found as usual by the Maxwell construction.

The two procedures outlined above represent two extreme situations, which are both not realized in nature, for an isolated heated nucleus. The equilibrium case assumes a pressure equilibrium between an external gas of nucleons and the nucleus. The presence of the external gas is assumed, in order to be able to perform an equilibrium calculation, but has no physical counterpart in an experiment with isolated nuclei. The metastable case assumes zero external pressure, which might seem more reasonable, but is strictly not accessible in a static variational calculation except by our boundary conditions above, and by cutting the solutions $\rho_q(r)$ at $r = R$ (see sect. 2.1 for the details). It is conceivable, that the physical situation lies somewhere in between these two extreme models. A hot nucleus is evaporating nucleons (mostly neutrons), which exert a pressure on the surface of the nucleus, due to momentum conservation. This pressure is of course smaller than the pressure corresponding to an external gas, but it might well be non-zero.

2.1. THE CASE OF A METASTABLE NUCLEUS

We shall now discuss the variational equation (2.1) in the metastable situation, $P_0 = 0$, for spherical nuclei. A free variation of the profiles $\rho_q(r)$ at $T > 0$ will lead to solutions with the same qualitative structure as in the semi-infinite case [8]): at the center, the densities start from some initial values $\rho_q(0) = \rho_{0q}$ with zero slopes (for parity reasons), i.e. $\rho_q'(0) = 0$. At some finite distance R_q from the center, the density ρ_q has a minimum, i.e. $\rho_q'(R_q) = 0$, with $\rho_q(R_q) = \rho_{gq} > 0$. We shall assume that $R_p = R_n = R$ and identify the sphere with radius R with the surface of the metastable nucleus. Note that R is given variationally and *not* imposed from the outside.

The situation may be visualized by a liquid drop enclosed by moving walls, i.e. by a piston whose wall (the sphere at $r = R$) is adjusted at each temperature such that the pressure P_0 is zero inside. This is exactly the way one might produce superheated liquid drops, as discussed in ref. [7]) for instance. For the free metastable nucleus under discussion here, the piston wall (i.e. the spherical box with radius R) has no physical meaning; it is merely an equivalent picture, a technical device to create the boundary condition $P_0 = 0$. That this system is, indeed, evaporating nucleons can be seen from the fact that the intrinsic pressure at $r = R$ is non-zero and thus gives the nucleons an (initial) radial escape velocity (see the discussion in sect. 4.2 below).

The metastable boundary conditions can thus by summarized by

$$P_0 = 0\,, \qquad \rho_q'(0) = \rho_q'(R) = 0\,, \qquad (q = n, p)\,. \tag{2.2}$$

As in the semi-infinite case [8,10]), we keep only the parts of the solutions $\rho_q(r)$ of eq. (2.1) with $r \leq R$. The upper limit of the radial integral in eq. (2.1) is thus $r_{max} = R$. We emphasize again that R is a variational parameter which results from the solution of eqs. (2.1) and (2.2). For practical reasons, we perform the variation in (2.1) in two steps: (i) variation of $\rho_q(r)$ with fixed R, and (ii) variation of R with fixed shapes $\rho_q(r)$.

Performing the variations for fixed R leads to the coupled differential equations

$$\frac{\delta}{\delta\rho_q}\left(\mathcal{F}[\rho_n, \rho_p] + \mathcal{E}_C[\rho_p]\right) = \lambda_q\,, \qquad (q = n, p) \tag{2.3}$$

where we have now explicitly included the Coulomb energy density $\mathcal{E}_C[\rho_p]$. Variation with respect to R gives the additional boundary condition

$$\mathcal{F}[\rho_n(R), \rho_p(R)] = \lambda_n\rho_n(R) + \lambda_p\rho_p(R) - \tfrac{1}{2}\rho_p(R)\,V_p(R)\,, \tag{2.4}$$

where $V_p(r)$ is the Coulomb potential (2.5) (note that $P_0 = 0$). The chemical potentials λ_q must be iterated to get the correct particle numbers N for neutrons and Z for protons inside the sphere with radius R. For the symmetric case ($\rho_n = \rho_p = \frac{1}{2}\rho$) without Coulomb interaction in the semi-infinite limit, i.e. $N = Z = \frac{1}{2}A$ towards infinity, we obtain the case studied in refs. [8,10]). (In this case, $\lambda_n = \lambda_p = \lambda$ is just the volume energy, i.e. the binding energy per particle of infinite nuclear matter).

The variation of the Coulomb energy density $\mathcal{E}_C$ gives the Coulomb potential for protons ($q = p$) and zero for neutrons ($q = n$).

$$V_q(\boldsymbol{r}) \equiv \frac{\delta\mathcal{E}_C[\rho_p]}{\delta\rho_q} = \delta_{q,p}\,e^2 \int \mathrm{d}^3r'\,\rho_p(\boldsymbol{r}')/|\boldsymbol{r} - \boldsymbol{r}'|\,. \tag{2.5}$$

We separate the nuclear free-energy density $\mathcal{F}$ as a sum, using the SkM* force, as

$$\mathcal{F} = \mathcal{F}_W + \mathcal{F}_\tau + \mathcal{F}_s\,, \tag{2.6}$$

with the contributions

$$\mathcal{F}_{\mathrm{W}} = \beta_{\mathrm{W}} \sum_{\mathrm{q=r,p}} h_{\mathrm{q}} \xi_{\mathrm{q}} (\nabla \rho_{\mathrm{q}})^2 / \rho_{\mathrm{q}} , \tag{2.7}$$

$$\mathcal{F}_{\nabla} = \nabla \rho_{\mathrm{n}} \nabla \rho_{\mathrm{p}} c_0 + \tfrac{1}{2} c_1 \sum_{\mathrm{q=n,p}} (\nabla \rho_{\mathrm{p}})^2 , \tag{2.8}$$

$$\mathcal{F}_{\infty} = \mathcal{E}^{\infty}_{\mathrm{pot}} + \sum_{\mathrm{q=n,p}} (T \eta_{\mathrm{q}} \rho_{\mathrm{q}} - \tfrac{3}{2} A_{\mathrm{q}} T J_{3/2}(\eta_{\mathrm{q}})) , \tag{2.9}$$

$$\mathcal{E}^{\infty}_{\mathrm{pot}} = c_8(\rho_{\mathrm{n}}^2 + \rho_{\mathrm{p}}^2) + c_4 \rho_{\mathrm{n}} \rho_{\mathrm{p}} + \tfrac{1}{2} c_0 (\rho_{\mathrm{n}} + \rho_{\mathrm{p}})^{\alpha} (\rho_{\mathrm{n}}^2 + \rho_{\mathrm{p}}^2 + 4 \rho_{\mathrm{n}} \rho_{\mathrm{p}}) . \tag{2.10}$$

The constants c_i are combinations of the parameters of the SkM* force and are listed in appendix A, together with α. The function ξ_{q} appearing in eq. (2.7) is defined as [10])

$$\xi_{\mathrm{q}} = \tfrac{1}{12} J_{1/2}(\eta_{\mathrm{q}}) J_{-3/2}(\eta_{\mathrm{q}}) J^{-2}_{-1/2}(\eta_{\mathrm{q}}) \tag{2.11}$$

in terms of the Fermi integrals

$$J_{\mu}(\eta) = \int_0^{\infty} \mathrm{d}y \frac{y^{\mu}}{1 + \exp(y - \eta)} \tag{2.12}$$

and the temperature (T) dependent function A_{q} is defined as

$$A_{\mathrm{q}} = \frac{1}{2n^2} (T / h_{\mathrm{q}})^{3/2} , \tag{2.13}$$

where h_{q} contains the effective-mass correction to the nucleon mass m as

$$h_{\mathrm{q}} = \frac{\hbar^2}{2m} + c_7 \rho_{\mathrm{q}} + c_2 \rho_{\mathrm{q}} , \qquad (\mathrm{q} = \mathrm{n, p \text{ and } } \bar{\mathrm{q}} = \mathrm{p, n}) \tag{2.14}$$

(see appendix A for the constants c_i). The quantity η_{q} is related to the density ρ_{q} by

$$\rho_{\mathrm{q}} = A_{\mathrm{q}} J_{1/2}(\eta_{\mathrm{q}}) . \tag{2.15}$$

We have included a factor $\beta_{\mathrm{W}} \sim 1.4$ in eq. (2.7) to correct the Weizsäcker term for the omission of fourth-order terms in the free-energy density, which one obtains in the extended Thomas-Fermi (ETF) model [10]) (see the discussion in sect. 5.1). We omit also the spin-orbit term in the free-energy density. In addition, we neglect terms arising from gradients of the effective mass. (The spin-orbit and mass-gradient terms are written out explicitly in appendix D.)

The variational equation (2.3) represents two coupled simultaneous second-order non-linear differential equations for the neutron and proton densities ρ_{n} and ρ_{p}. Assuming spherical symmetry of the nucleus, they read

$$\rho''_{\mathrm{q}}(r) = \frac{c_{\mathrm{q}}[\beta_{\bar{\mathrm{q}}}(r) + V_{\bar{\mathrm{q}}}(r)] + \beta_{\bar{\mathrm{q}}}(r)[\beta_{\mathrm{q}}(r) + V_{\mathrm{q}}(r)]}{c_{\mathrm{q}}^2 - B_{\bar{\mathrm{q}}}(r) B_{\mathrm{q}}(r)} , \tag{2.16}$$

where $\bar{\mathrm{q}} = \mathrm{p}$ if $\mathrm{q} = \mathrm{n}$ and vice versa. The constants c_{q} have the value $c_{\mathrm{n}} = c_{\mathrm{p}} = c_0$ (see appendix A) and the functions $B_{\mathrm{q}}(r)$ contain both $\rho_{\mathrm{n}}(r)$ and $\rho_{\mathrm{p}}(r)$ whereas the

functions $\beta_q(r)$ contain the first derivatives $\rho_n'(r)$ and $\rho_p'(r)$, in addition. They are defined in appendix B.

The equations were solved numerically using a Runge-Kutta method and the CERN library routine COLSYS for comparison. Special care has to be taken at $r = 0$ and for vanishing denominator in eq. (2.16). The necessary limiting procedures are described in appendix C.

2.2. THE EQUILIBRIUM CASE

In ref. [3]) the heated nucleus was assumed to be embedded in a gas of infinite extension, which exerts a finite pressure on the nucleus in order to allow thermodynamic equilibrium. Then the thermodynamic potential of the gas alone (at density ρ_G) is subtracted, so the properties of the nucleus alone (density ρ_{NG}) are supposedly isolated. Since in such a subtraction procedure the Coulomb interaction energy still would diverge, due to the infinite gas background, the authors of ref. [3]) propose to write the total subtracted thermodynamic potential density $\tilde{\omega}$ including the Coulomb energy density $\mathscr{E}_C$ as

$$\tilde{\omega} = \omega(\rho_{NG}) - \omega(\rho_G) + \mathscr{E}_C(\rho_{NG} - \rho_G) \,. \tag{2.17}$$

This means, that only the Coulomb energy of the density *difference* $\rho_{NG} - \rho_G$ is taken into account; this energy is finite.

The variation of the subtracted thermodynamic potential leads in this way to four coupled differential equations of the same structure as eq. (2.16), for the four density profiles $\rho_{NGn}, \rho_{NGp}, \rho_{Gn}, \rho_{Gp}$. Only the Coulomb term V_q has to be redefined as

$$V_q^{NG} = V_q^G = 4\pi e^2 \left(\frac{1}{r} \int_0^r \mathrm{d}r'\, r'^2 (\rho_{NGp} - \rho_{Gp}) + \int_r^R \mathrm{d}r'\, r' (\rho_{NGp} - \rho_{Gp}) \right) \delta_{q,p} \,. \tag{2.18}$$

Due to the presence of the Coulomb term, all four differential equations are coupled. If the Coulomb interaction is turned off, the four equations decouple to two sets of two coupled equations for ρ_{NGn}, ρ_{NGp} and ρ_{Gn}, ρ_{Gp}. These equations were solved numerically in ref. [4]). In our present work, we used a Runge-Kutta method to obtain the solutions.

3. Energies of giant resonances

One possible way to see the effect of temperature experimentally may be the measurement of giant resonances (GR). Using a scaling procedure, the authors of ref. [11]) derive expressions for various multipole GR energies in terms of Skyrme forces.

The Skyrme energy functional E can be separated into several parts, according to their scaling behavior,

$$E = E_\delta + E_\rho + E_{\mathrm{fin}} + \bar{E}_{\mathrm{kin}} + \bar{E}_{\mathrm{s.o.}} + E_C \,, \tag{3.1}$$

with

$$E_\delta = \int \mathrm{d}^3r\, (c_8(\rho_\mathrm{n}^2+\rho_\mathrm{p}^2)+c_4\rho_\mathrm{n}\rho_\mathrm{p})\,, \tag{3.2}$$

$$E_\rho = \int \mathrm{d}^3r\, \tfrac{1}{2}c_6(\rho_\mathrm{n}+\rho_\mathrm{p})^\alpha(\rho_\mathrm{n}^2+\rho_\mathrm{p}^2+4\rho_\mathrm{n}\rho_\mathrm{p})\,, \tag{3.3}$$

$$E_\mathrm{fin} = \int \mathrm{d}^3r\, (\tfrac{1}{2}c_1[(\nabla\rho_\mathrm{n})^2+(\nabla\rho_\mathrm{p})^2]+c_0\nabla\rho_\mathrm{n}\nabla\rho_\mathrm{p}$$

$$+c_7(\tau_\mathrm{n}\rho_\mathrm{n}+\tau_\mathrm{p}\rho_\mathrm{p})+c_2(\tau_\mathrm{n}\rho_\mathrm{p}+\tau_\mathrm{p}\rho_\mathrm{n}))\,, \tag{3.4}$$

$$\bar{E}_\mathrm{kin} = \int \mathrm{d}^3r \frac{\hbar^2}{2m}(\tau_\mathrm{n}+\tau_\mathrm{p})\,, \tag{3.5}$$

$$\bar{E}_\mathrm{s.o.} = \int \mathrm{d}^3r\, (-\tfrac{1}{8}W_0^2 \sum_{\mathrm{q}=\mathrm{n,p}} h_\mathrm{q}^{-1}\rho_\mathrm{q}(2\nabla\rho_\mathrm{q}+\nabla\rho_{\bar{\mathrm{q}}})^2)\,, \tag{3.6}$$

$$E_\mathrm{C} = \frac{\mathrm{e}^2}{2}\int \mathrm{d}^3r_1\, \mathrm{d}^3r_2\, \rho_\mathrm{p}(r_1)\rho_\mathrm{p}(r_2)\frac{1}{|\boldsymbol{r}_1-\boldsymbol{r}_2|}\,, \tag{3.7}$$

where the quantity τ_q, related to the kinetic energy (excluding effective-mass and spin-orbit terms) is

$$\tau_\mathrm{q} = h_\mathrm{q}^{-1}A_\mathrm{q}TJ_{3/2}(\eta_\mathrm{q})+\beta_\mathrm{W}\mathcal{C}_\mathrm{q}\frac{(\nabla\rho_\mathrm{q})^2}{\rho_\mathrm{q}}+\tfrac{1}{3}\Delta\rho_\mathrm{q}\,, \tag{3.8}$$

with

$$\mathcal{C}_\mathrm{q} = \tfrac{5}{2}\xi_\mathrm{q}-36\xi_\mathrm{q}^2+w_\mathrm{q}\,, \tag{3.9}$$

$$w_\mathrm{q} = \tfrac{3}{8}J_{1/2}^2(\eta_\mathrm{q})J_{-5/2}(\eta_\mathrm{q})J_{-1/2}^3(\eta_\mathrm{q})\,. \tag{3.10}$$

Eqs. (3.2)-(3.7) correspond to the energies given explicitly in ref. [11]) but are generalized to two different densities for ρ_n and ρ_p. Then the monopole GR ("breathing mode") energy becomes

$$E_3(L=0) = \left(\left(\frac{\hbar^2}{Am\langle r^2\rangle}\right)(4\bar{E}_\mathrm{kin}+9E_\delta+25(E_\mathrm{fin}+\bar{E}_\mathrm{s.o.})+(3\alpha+3)^2E_\rho)\right)^{1/2}, \tag{3.11}$$

and the quadrupole GR energy is

$$E_3(L=2) = \left(\left(\frac{4\hbar^2}{Am\langle r^2\rangle}\right)(\bar{E}_\mathrm{kin}+E_\mathrm{fin}+\tfrac{1}{4}E_\mathrm{s.o.}-\tfrac{1}{5}E_\mathrm{C})\right)^{1/2}, \tag{3.12}$$

where $\langle r^2\rangle$ is the mean square radius of the nucleus. The compressibility of the finite nucleus is expressed as

$$\kappa = (4\bar{E}_\mathrm{kin}+9E_\delta+25(E_\mathrm{fin}+\bar{E}_\mathrm{s.o.})+(3\alpha+3)^2E_\rho)/A\,. \tag{3.13}$$

The bar above $\bar{E}_{\rm kin}$ is to emphasize the fact that it is not the full kinetic energy, since the part coming from the effective-mass correction is already contained in $E_{\rm fin}$ (the $\tau\rho$ terms) and the kinetic spin-orbit part is contained in $\bar{E}_{\rm s.o.}$, which is therefore also marked with a bar. Note that we have explicitly taken the neutron and proton densities separately into account.

The full total energy (up to second-order density gradients) contains additional terms in the sum eq. (3.1), denoted by E^*, due to the gradients of $h_{\rm q}$,

$$E^* = \int {\rm d}^3 r \sum_{\rm q=n,p} \nabla h_{\rm q} (\nabla h_{\rm q} h_{\rm q}^{-1} \rho_{\rm q} (\tfrac{9}{4}\mathcal{C}_{\rm q} - \tfrac{7}{48}) + \nabla \rho_{\rm q} (3\mathcal{C}_{\rm q} - \tfrac{5}{12}) + \tfrac{1}{3}\nabla \rho_{\rm q}) \,. \tag{3.14}$$

Gradients of the effective mass are not considered here, since they represent only a minor correction to the GR energies [12]); in addition, these terms have semiclassically a wrong scaling behavior.

4. Thermal quantities of a heated nucleus

4.1. THE ENTROPY

The entropy density, including gradients of the effective mass, reads

$$\sigma = \sum_{\rm q=n,p} \left(\tfrac{5}{3} A_{\rm q} J_{3/2}(\eta_{\rm q}) - \eta_{\rm q}\rho_{\rm q} - \frac{\nu_{\rm q}}{T} \left[\beta_{\rm W} h_{\rm q} \frac{(\nabla \rho_{\rm q})^2}{\rho_{\rm q}} + \tfrac{9}{4} (\nabla h_{\rm q})^2 h_{\rm q}^{-1} \rho_{\rm q} + 3 \nabla h_{\rm q} \nabla \rho_{\rm q} \right] \right) , \tag{4.1}$$

where we have again included a factor $\beta_{\rm W} \sim 1.4$ as in eq. (2.7), so the relation $\sigma = -\partial \mathcal{F}/\partial T$ still holds true.

4.2. THE NEUTRON EVAPORATION TIME

We follow an argument given in ref. [2]). The evaporation time τ is related to the neutron density $\rho = n/{\rm vol}$ (occupation number per volume), the neutron capture cross section $\sigma_{\rm c}$ and the velocity v of the neutrons via [13])

$$\frac{1}{\tau} = \overline{\rho \sigma_{\rm c} v} \,, \tag{4.2}$$

where the bar denotes an average over neutron states, with spin degeneracy $g = 2$. From phase-space considerations we have that ${\rm vol} \times {\rm d}^3 p = h^3$ (h is Planck's constant), and assuming spherical symmetry the density is expressed as

$$\rho = \frac{n}{h^3} 4\pi p^2 \, {\rm d}p \,. \tag{4.3}$$

With $E = p^2/2{\rm m}$, one gets

$$\rho s v = 4\pi \sigma_{\rm c} \frac{n}{h^3} p^2 \, {\rm d}p \frac{p}{m} = 4\pi \sigma_{\rm c} \frac{n}{h^3} 2mE \, {\rm d}E \,, \tag{4.4}$$

with m being the neutron mass, the average is then

$$\frac{1}{\tau} = 4\pi g \frac{2m}{h^3} \int \mathrm{d}E\, E \sigma_c n \tag{4.5}$$

(compare this also to the Weisskopf evaporation formula, see e.g. ref. [14]).

Assuming σ_c to be equal to the geometrical cross section of a spherical nucleus with radius R, $\sigma_c = \pi R^2$ and approximating the occupation number for fermions as

$$n(E) = \left(1 + \exp\left(\frac{E - \lambda_n}{T}\right)\right)^{-1} \sim \exp\frac{\lambda_n - E}{T}, \tag{4.6}$$

the integration in eq. (4.7) can be performed analytically. The evaporation time for neutrons is thus

$$\tau[\lambda_n] = \left(\frac{4\mathrm{m}}{\hbar^2 h}(RT)^2 \exp\frac{\lambda_n}{T}\right)^{-1}. \tag{4.7}$$

Here, λ_n is the chemical potential for neutrons, T is the temperature and $\hbar = h/2\pi$.

One should be aware of the fact that the above derivation of the evaporation time assumes an equilibrated gas phase with occupation numbers given by eq. (4.6). In a metastable calculation, however, the chemical potential λ_n which enters into the variational eq. (2.1) is not equal to the equilibrium value λ_{eq} corresponding to the gas density at the boundary. Therefore, we shall be calculating the evaporation times for the metastable nucleus using $\lambda_n = \lambda_{eq}$, with the chemical potential of the gas phase at density ρ_g given by

$$\lambda_{eq} = \left.\frac{\partial F_\infty}{\partial \rho_n}\right|_{\rho_n = \rho_g}. \tag{4.8}$$

Since the evaporation times in the above formulation are ambiguous with respect to the choice of the chemical potential, we recur to an alternate approach, in which only the density ρ_g of the gas phase enters. Consider the rate $\mathrm{d}N/\mathrm{d}t$ of evaporated neutrons. The radial flux $\rho_g \bar{v}_{rad}$ is related to the rate via

$$\mathrm{d}N/\mathrm{d}t = \tau^{-1} = 4\pi R^2 \rho_g \bar{v}_{rad}. \tag{4.9}$$

Here, R is again the radius defining the nuclear surface and $\bar{v}_{rad}$ is the mean *radial* velocity. It is important to calculate $\bar{v}_{rad}$ correctly. Since it is the kinetic energy distribution which allows the particles to "knock at the wall" of the nuclear surface, we write

$$\bar{v}_{rad} = \sqrt{\langle v_{rad}^2 \rangle} = \sqrt{\tfrac{1}{3}\langle p^2/m^2 \rangle} = \sqrt{\tfrac{2}{3}\langle E_{kin} \rangle}. \tag{4.10}$$

The factor $\frac{1}{3}$ comes from the fact that the 2 angular degrees of freedom do not contribute to the radial flux. Since

$$\langle E_{kin} \rangle = \frac{D}{h^3} \int \mathrm{d}^3 p \frac{p^2}{2m} n(p)/\rho_g, \tag{4.11}$$

with the fermion occupation numbers $n(p) \equiv n\{E(p)\}$ and with $\rho_g = A_n J_{1/2}(\eta_n)$ (see eq. (2.15)), we obtain

$$\langle E_{kin} \rangle = T J_{3/2}(\eta_n)/J_{1/2}(\eta_n) \tag{4.12}$$

[Using the low density, i.e. $\eta < 0$, expansion [10]) $J_\mu(\eta) \sim \Gamma(\mu+1)e^\eta$, this yields the well-known ideal gas result $\langle E_{kin} \rangle = \frac{3}{2}T$]. The expression for the evaporation time thus becomes

$$\tau[\rho_g] = (4\pi R^2 \rho_g)^{-1} \left(\frac{2TJ_{3/2}(\eta_n)}{3mJ_{1/2}(\eta_n)} \right)^{1/2}. \tag{4.13}$$

5. Results for uncharged lead

5.1. SIMULATION OF THE MISSING FOURTH-ORDER TERMS

As mentioned in sect. 2.1 we include a factor β_W in the Weizsäcker term of the free-energy density to simulate the omission of fourth-order gradient terms which appear in the ETF model and are known [10,15]) to give non-negligible contributions to the nuclear binding energies. This procedure has been proposed in ref. [15]): a factor $\beta_W = 1.4$ is suited best to correct the calculated energies, whereas $\beta_W = 4$ adjusts the density profiles and root-mean-square (r.m.s.) radii to correspond to those calculated with the inclusion of fourth-order terms. To show the influence of β_W on various energies and the density profiles, we performed a test calculation for an uncharged metastable $A = 208$ nucleus (uncharged lead), for the values $\beta_W = 1.0$, 1.4 and 4.0. Fig. 1 displays the density profiles at temperatures $T = 3$, 5 and 10 MeV. (Note that *uncharged* lead is still stable up to $T > 11$ MeV in these calculations.) The difference in shape between $\beta_W = 1$ and $\beta_W = 4$ is almost invisible at 3 MeV temperature. For higher temperatures, the difference between $\beta_W = 1$ and $\beta_W = 1.4$ also stays minimal, whereas the shapes for $\beta_W = 4$ have a longer tail and a smaller central density. The corresponding neutron evaporation times, r.m.s. radii, entropies, compressibilities and binding energies are compiled in table 1. The neutron evaporation times do not differ appreciably by changing the value of β_W. The entropy and the r.m.s. radius increase, the compressibility decreases, and the binding energy becomes less negative with increasing β_W, but the differences between $\beta_W = 1.0$ and $\beta_W = 1.4$ stay small. This demonstrates the fact that the fourth-order terms in the free energy, simulated by $\beta_W = 1.4$, represent really a small correction. (We will not consider the case $\beta_W = 4$ any further.)

5.2. CASE STUDY: METASTABLE VERSUS EQUILIBRIUM NUCLEUS

We shall now discuss and compare some results obtained with the two schemes for describing hot nuclei. In fig. 2 we present the density profiles of uncharged lead in both the metastable and equilibrium cases at a temperature $T = 3$ MeV. Also

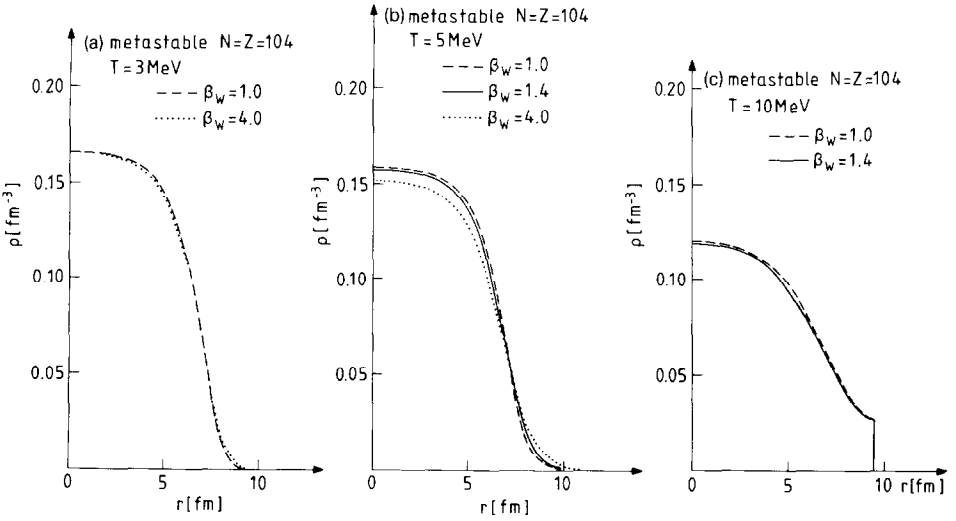

Fig. 1. The effect of the Weizsäcker correction coefficient β_W on the density profile of an uncharged metastable $N = Z = 104$ nucleus at three values of the nuclear temperature T. At $T = 3$ MeV the profile calculated with $\beta_W = 1.4$ is not distinguishable from the dashed line with $\beta_W = 1$.

included is a calculation, in which the density is parametrized as a Fermi-like function [16])

$$\rho(r) = \rho_0 \left(\frac{1 + \cos(R_0/\alpha)}{\cosh(r/\alpha) + \cosh(R_0/\alpha)} \right)^{\gamma}, \tag{5.1}$$

with the parameters ρ_0, α and γ, which minimize the free energy. In this calculation neither external gas nor boundary are present; the constraint resides in the parametrized form of the density, which drops to zero outside of the nucleus. As long

TABLE 1

The effect of the Weizsäcker coefficient β_W at different temperatures T on the total energy per particle E/A, entropy per particle S/A, incompressibility κ, the evaporation times $\tau[\lambda_{eq}]$ and $\tau[\rho_g]$ (as defined in sect. 4.2), and the r.m.s. radius $\langle r^2 \rangle^{1/2}$. The calculations are for an uncharged $N = Z = 104$ metastable nucleus

T [MeV]	β_W	E/A [MeV]	S/A	κ [MeV]	$\tau[\lambda_{eq}]$ [10^{-23} s]	$\tau[\rho_g]$ [10^{-23} s]	$\sqrt{\langle r^2 \rangle}$ [fm]
3	1.0	−11.68	0.512	150	286	110	5.54
3	1.4	−11.51	0.515	149	286	111	5.54
3	4.0	−10.50	0.526	145	286	110	5.59
5	1.0	−10.21	0.854	134	19.1	5.62	5.68
5	1.4	−10.00	0.873	128	19.1	5.60	5.73
5	4.0	−8.57	1.000	102	17.9	5.54	6.00
10	1.0	−2.93	1.781	68	3.08	0.190	6.55
10	1.4	−2.66	1.805	65	3.03	0.193	6.58

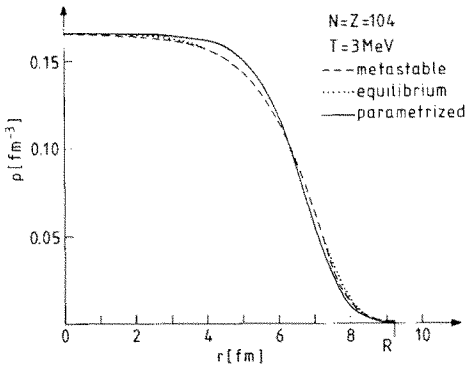

Fig. 2. Different model calculations for an uncharged $N = Z = 104$ nucleus at the temperature $T = 3$ MeV. The density profile of the metastable nucleus (zero external pressure, dashed line) ends at the boundary R. The dotted line corresponds to a nucleus in an external gas of finite density and pressure. The full line represents a Fermi-function-like parametrization of the density, see sect. 5.2.

as the temperature T is not too high, both the metastable and equilibrium cases yield very small densities at the boundary or of the gas, respectively, and the Fermi-function-like parametrization is expected to make sense. [From $T \sim 5$ MeV on, there exist no parametrized solutions [16,17]) because the density must not drop to zero outside of the nucleus at higher temperatures, if the system is to be stable.] Fig. 2 shows that the metastable and equilibrium cases are almost indistinguishable at $T = 3$ MeV. The calculation using the parametrization (5.1) gives also a comparable density profile.

Table 2 lists various quantities at $T = 3$ and 10 MeV. At $T = 3$ MeV, the binding energy, entropy, compressibility and evaporation time are somewhat lower in the

TABLE 2

Different model calculations at $T = 3$ MeV and $T = 10$ MeV. The model situations are: metastable nucleus with no external pressure, equilibrium nucleus in an external gas, a Fermi function like parametrization of the density profile, and a subtraction procedure as explained in sect. 5.2, all for an uncharged $N = Z = 104$ nucleus. Quantities shown are as in table 1.

Type	E/A [MeV]	S/A	κ [MeV]	$\tau[\rho_g]$ [10^{-23} s]	$\sqrt{\langle r^2 \rangle}$ [fm]
(a) $T = 3$ MeV					
metastable	−11.7	0.512	150	110	5.54
equilib.	−13.2	0.503	146	287	5.53
parametr.	−13.1	0.429	169	-	5.46
subtract.	−11.7	0.507	151	-	5.53
(b) $T = 10$ MeV					
metastable	−2.93	1.781	68	0.190	6.55
equilib.	−5.28	1.454	92	0.621	6.45

equilibrium case than in the metastable case, whereas the r.m.s. radii stay roughly the same. This is also found at $T = 10$ MeV with the exception of the compressibility, which does not become as small in the equilibrium case as in the metastable case. A hot metastable nucleus is thus softer than the corresponding equilibrium nucleus. The metastability reflects itself in the behavior of the other quantities in table 2. The parametrized calculation has the same binding energy as the equilibrium one; the other quantities differ from both the metastable and equilibrium ones. In particular, the entropy is much lower. We include in the table also a comparison with a simplified subtraction procedure, in which the functionals are all calculated as integrals over the subtracted density $\rho_{NG} - \rho_G$ as in the Coulomb energy part of eq. (2.16). This subtraction should be closer in spirit to the parametrized density profiles, since in both cases the densities drop to zero outside of the nucleus. However, the parametrized solutions still differ from the ones obtained with the simplified subtraction scheme. In fact, the simplified subtraction procedure yields results close to the metastable values, when the temperature is low ($T = 3$ MeV).

In the next figure (fig. 3) we explore the dependence of the entropy on the model used. Fig. 3a displays the entropies of the metastable, equilibrium and parametrized cases, as functions of the temperature. Also shown are results of a Hartree-Fock (HF) calculation for a nucleus in a gas background from ref. [3]); they are to be compared with caution, however, since the Skyrme force used is different and since we did the calculation for a $N = Z = 104$ nucleus, whereas the HF results are for uncharged lead with $N = 126$, $A = 82$. Since the notion of temperature being model

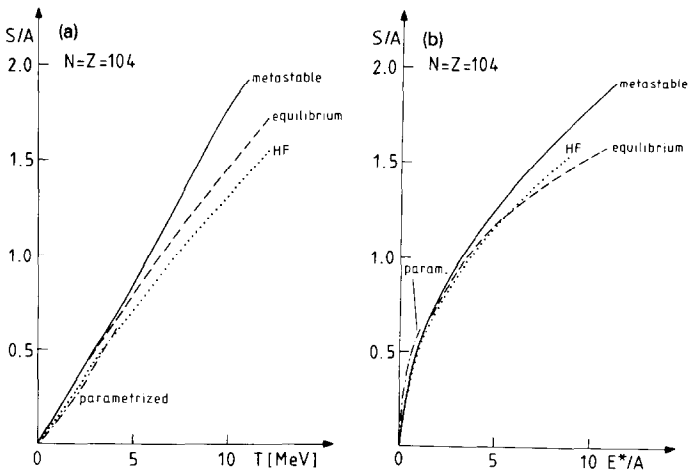

Fig. 3. (a) The entropy per particle S/A as a function of the temperature T. The metastable (full line), parametrized (dash-dotted) and equilibrium (dashed) calculations are for an uncharged $N = Z = 104$ nucleus, whereas the Hartree-Fock curve for a nucleus in an external gas (HF, dotted line) is for uncharged ^{208}Pb with a somewhat different Skyrme force. (b) The entropy per particle as in (a), but plotted versus the excitation energy per particle E^*/A.

dependent is not really a physical one, we also plot the entropy versus the excitation energy E^* in fig. 3b. To get E^*, we had to calculate the reference energies at $T = 0$ as well, taking the proper $T \to 0$ limits in all temperature-dependent expressions. As functions of the temperature at $T \leqslant 5$ MeV, the metastable and equilibrium solutions are very close and differ from the HF calculation (fig. 3a). The parametrized solution follows somewhat the HF line, but has a different curvature. For $T \geqslant 5$ MeV (where the parametrized solutions do not exist), the metastable case exhibits a stronger increase of the entropy, compared to both equilibrium and HF. As a function of the excitation energy, the entropy behaves differently. Fig. 3b shows that the equilibrium and HF cases are quite close now - a confirmation of the fact that the approach used in the present work is a reasonable approximation to the quantum mechanical HF clculation. The entropy of the metastable solution rises still faster than the equilibrium or HF ones. The result of the parametrized case does not agree with the HF curve anymore and has the fastest increase.

The evaporation times for neutrons are calculated according to the procedures of sect. 4.2 and depicted in fig. 4 as functions of the temperature. The equilibrium calculation yields evaporation times $\tau[\rho_g]$ (calculated according to eq. (4.13)) which are a factor 3 larger than in the metastable situation, since the external gas exerts a pressure on the nucleus, making it more stable than under zero-pressure conditions. In both cases, we have used the same nuclear radius R to concentrate on the effect of different gas densities only. Included in fig. 4 is also $\tau[\lambda_{eq}]$ for the metastable case [calculated with eqs. (4.7) and (4.8)]; it is about 3 times larger than $\tau[\rho_g]$ for

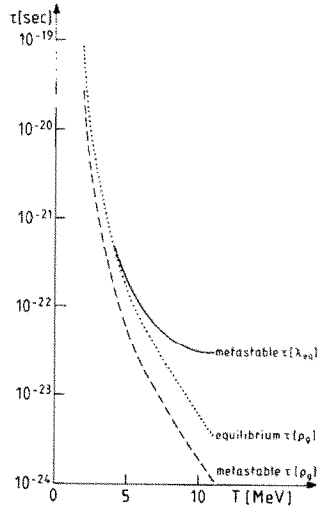

Fig. 4. The neutron evaporation times as functions of the temperature T. The equilibrium calculation of $\tau[\rho_g]$ (dotted line) is to be compared to the dashed metastable curve for $\tau[\rho_g]$. The full line for $\tau[\lambda_{eq}]$ (metastable nucleus) runs close to the dotted line at low temperatures and is to be compared to the metastable calculation of $\tau[\rho_g]$ (dashed line).

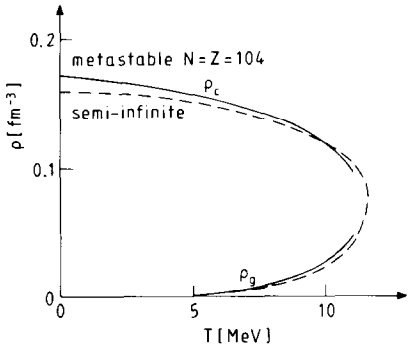

Fig. 5. The central density ρ_c and the "gas" density ρ_g at the surface of an uncharged metastable $N = Z = 104$ nucleus versus the temperature T (full line). The dashed curve represents the corresponding "liquid" and "gas" densities obtained for semi-infinite nuclear matter.

small temperature and becomes more than one order of magnitude larger at high T. We do not attempt here to extract τ from the HF results of ref. [3]), since τ is sensitive to the neutron density (or chemical potential), and our test nucleus with $N = Z = 104$ differs from the uncharged lead nucleus with $N = 126$, $Z = 82$ used in ref. [3]).

5.3. THE CRITICAL TEMPERATURE

The highest temperature at which a stable solution for a nucleus is found can be compared to the critical temperature in a semi-infinite calculation. In fig. 5 the densities of the gas and liquid phases of a semi-infinite system taken from ref. [10]) are drawn together with the gas and central densities of the metastable nucleus, as functions of the temperature. Both calculations were performed with the same Skyrme force and the boundary conditions of the metastable situation. Contrary to the semi-infinite system, where the gas and liquid densities meet at the critical temperature and a single phase is formed, the metastable solutions break down before the corresponding densities become the same, due to finite size effects. The critical temperature in the metastable case, the flash temperature, is found to be a little more than 11 MeV for an uncharged $A = 208$ nucleus.

6. Metastable ^{208}Pb

Including the Coulomb energy in the calculation of the metastable nucleus has a dramatic effect on the solutions. Fig. 6 shows the neutron and proton density profiles of metastable ^{208}Pb at two different temperatures, $T = 2$ and 4 MeV. The density $\rho(R)$ at the boundary is much bigger than the corresponding density in the

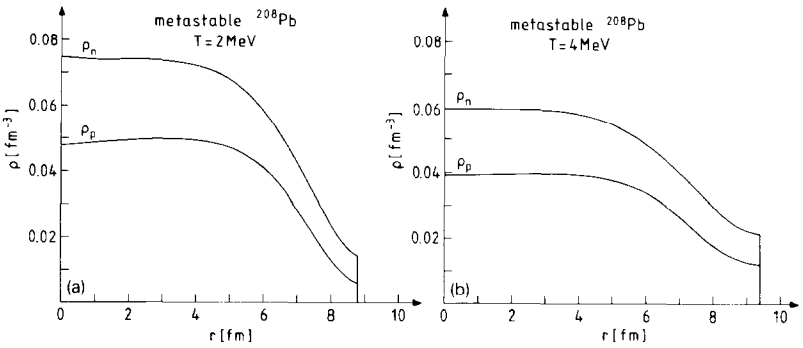

Fig. 6. The density profiles of neutrons (ρ_n) and protons (ρ_p) of metastable (charged) ^{208}Pb at temperatures $T = 2$ and 4 MeV.

uncharged case at the same temperature. The Coulomb energy has the effect of pushing nuclear matter towards the periphery of the nucleus. The flash temperature lies already at $T_m \sim 5$ MeV, i.e. no solution is found at this temperature anymore. The temperature range of the solutions is much shorter than the one in the uncharged case. In fact, the solutions at $T = 4$ MeV in the charged case resemble very much those at $T = 10$ MeV in the uncharged case.

The r.m.s. radii of an uncharged $N = Z = 104$ nucleus and of ^{208}Pb are depicted in fig. 7. At small T, they start off with a higher value and increase more steeply in the charged case than in the uncharged one. Although the r.m.s. radius of the latter is quite big at the flash temperature $T_m \geq 11$ MeV, it is likely that the r.m.s. radius of charged lead at its flash temperature $T_m \leq 5$ MeV is still bigger, since the curve

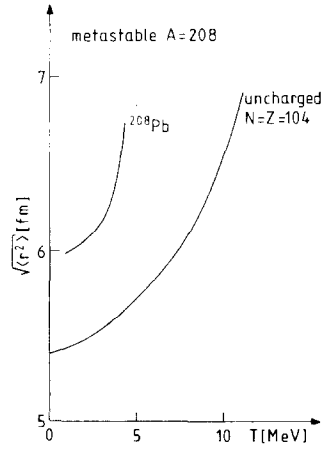

Fig. 7. The root-mean-square radius versus temperature for ^{208}Pb and for an uncharged $N = Z = 104$ nucleus, both calculated in the metastable situation.

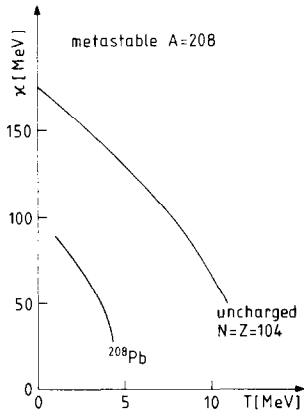

Fig. 8. The incompressibility κ of metastable ^{208}Pb and a metastable nucleus with $N = Z = 104$ as a function of the temperature.

for lead is very steep in the vicinity of T_m. In fig. 7 (and in our calculations) we have not come close enough to T_m to see this.

We compare in fig. 8 the incompressibilities κ. The incompressibility of the charged nucleus drops faster as a function of the temperature and is lower than for the uncharged nucleus. In both cases, however, κ drops by a factor of 3 to 4 in the range from low temperatures up to the flash temperature.

A set of quantities of interest is compiled in table 3. Since the temperature ranges are so different, we have selected $T = 3$, 5 and 10 MeV in the uncharged, and $T = 2$, 3 and 4 MeV in the charged case. As expected, the binding energy per nucleon E/A is not as negative for the charged nucleus, due to the repulsive Coulomb forces. (The fact that the value of E/A at $T = 4$ MeV is still quite negative for ^{208}Pb indicates again, that T_m lies closer to 5 MeV than to 4 MeV in the charged case, whereas

TABLE 3

Comparison between the metastable nuclei ^{208}Pb (charged) and uncharged $N = Z = 104$. In addition to the quantities of tables 1 and 2 we show the giant monopole resonance energy E_{GMR}

T [MeV]	E/A [MeV]	S/A	E_{GMR} [MeV]	κ [MeV]	$\tau[\lambda_{eq}]$ [10^{-23} s]	$\tau[\rho_g]$ [10^{-23} s]	$\sqrt{\langle r^2 \rangle}$ [fm]
(*a*) *uncharged* $N = Z = 104$							
3	−11.51	0.515	14.19	149	286	111	5.54
5	−10.00	0.873	12.74	128	19.1	5.60	5.73
10	−2.66	1.805	7.92	65	3.03	0.190	6.58
(*b*) *charged* ^{208}*Pb*							
2	−7.63	0.358	9.25	76	51.4	0.282	6.06
3	−6.58	0.575	8.11	61	17.8	0.228	6.18
4	−5.95	0.762	6.05	38	15.8	0.132	6.58

$T = 10$ MeV is closer to $T_m \sim 11$ MeV on the relative scale for the uncharged nucleus.) The entropy per particle S/A and the giant monopole resonance energy E_{GMR} are lower for the charged nucleus.

The evaporation times τ were calculated using the procedures described in sect. 4.2 and are also included in table 3. As in the uncharged situation, the values of $\tau[\lambda_{eq}]$ lie above those of $\tau[\rho_g]$, but $\tau[\lambda_{eq}]$ drops faster with increasing temperature in this case. (Compare the values at $T = 2$ MeV to the estimate obtained from the HF calculation of ref. [2]), where $\tau = 9 \times 10^{-21}$ s.) The equilibrium result is thus much above the metastable one.

7. Conclusions

We have studied hot nuclei in a semiclassical formalism, concentrating on the metastable situation where the external pressure is zero. A comparison to the equilibrium case in which the nucleus is surrounded by an external gas shows that the neutron evaporation times are shorter in the metastable case.

The Coulomb potential has a drastic effect on the solutions; nuclear matter is pushed somewhat away from the interior, considerably increasing the density at the periphery of the nucleus. The maximum temperature for which solutions exist in the metastable situation drops from above 11 MeV without Coulomb to below 5 MeV for the charged lead nucleus.

In the calculations for the equilibrium case [2-4]) (with subtraction of the gas background), the corresponding maximum temperature, obtained with a quite similar Skyrme force (SkM), was about 8 MeV. The difference to our ~5 MeV is clearly due to the missing external pressure in the metastable case. The real situation of a hot compound nucleus is presumably somewhere between these two extreme cases; we believe it to be closer to the present "metastable case". A maximum temperature of 5 MeV, which we expect not to increase more than by ~1 MeV for lighter nuclei, would be in good agreement with the fact that so far, no evidence has been established for the observation of temperatures higher than ~5-6 MeV of equilibrated compound nuclei created in heavy-ion collisions [18]).

The effect of increasing temperature is to increase the density at the border of the nucleus and to lower the binding energy and compressibility. Note that, quite naturally on the grounds of the present investigation, a weaker temperature dependence of GR energies was found in ref. [12]) where the parametrization (5.1) of the densities was used. A strong dependence of the compressibility and of the quadrupole GR energy on temperature could be exploited for an experimental determination of the temperature of excited nuclei, if it were possible to measure their GR energies.

We are very grateful to P. Gleissl and B. Hiller for many helpful discussions and to W. Stocker for his interest and fruitful conversations.

Appendix A

THE PARAMETERS OF THE SKYRME FORCE SkM*

Throughout this work, we use the SkM* parametrization of the Skyrme energy density

$$\begin{aligned} E_{\mathrm{SkM}^*} = {} & \tfrac{1}{2}t_0((1+\tfrac{1}{2}x_0)(\rho_\mathrm{n}+\rho_\mathrm{p})^2-(x_0+\tfrac{1}{2})(\rho_\mathrm{n}^2+\rho_\mathrm{p}^2))+\tfrac{1}{12}t_3\rho^\alpha(\rho_\mathrm{n}^2-\tfrac{1}{2}(\rho_\mathrm{n}^2+\rho_\mathrm{p}^2)) \\ & +\tfrac{1}{16}(3t_1-t_2)(\nabla\rho_\mathrm{n}+\nabla\rho_\mathrm{p})^2-\tfrac{1}{32}(3t_1+t_2)((\nabla\rho_\mathrm{n})^2+(\nabla\rho_\mathrm{p})^2) \\ & -\tfrac{1}{4}W_0^2\sum_{\mathrm{q}=\mathrm{n,p}}(h_\mathrm{q}^{-1}\rho_\mathrm{q}(\nabla\rho_\mathrm{q}+\nabla\rho_\mathrm{n}+\nabla\rho_\mathrm{p})^2+\tau_\mathrm{q}h_\mathrm{q}), \end{aligned} \tag{A.1}$$

where τ_q is related to the kinetic-energy density for neutrons or protons as

$$\begin{aligned} E_\mathrm{kin} = h_\mathrm{q}\tau_\mathrm{q} = {} & A_\mathrm{q}TJ_{3/2}(\eta_\mathrm{q})+\beta_\mathrm{w}h_\mathrm{q}(\nabla\rho_\mathrm{q})^2\rho_\mathrm{q}^{-1}\mathcal{O} \\ & +\tfrac{1}{8}h_\mathrm{q}^{-1}W_0^2\rho_\mathrm{q}(2\nabla\rho_\mathrm{q}+\nabla\rho_{\bar{\mathrm{q}}})+\tfrac{1}{3}h_\mathrm{q}\Delta\rho_\mathrm{q}, \end{aligned} \tag{A.2}$$

with

$$A_\mathrm{q} = \frac{1}{2\pi^2}(T/h_\mathrm{q})^{3/2}, \tag{A.3}$$

$$h_\mathrm{q} = \frac{\hbar^2}{2m}+c_7\rho_\mathrm{q}+c_2\rho_{\bar{\mathrm{q}}}, \tag{A.4}$$

$$\mathcal{O}_\mathrm{q} = \tfrac{5}{2}\xi_\mathrm{q}-36\xi_\mathrm{q}^2+\omega_\mathrm{q}, \tag{A.5}$$

$$\omega_\mathrm{q} = \tfrac{3}{8}J_{1/2}^2(\eta_\mathrm{q})J_{-5/2}(\eta_\mathrm{q})J_{-1/2}^{-2}(\eta_\mathrm{q}), \tag{A.6}$$

$$\xi_\mathrm{q} = -\tfrac{1}{12}J_{1/2}(\eta_\mathrm{q})J_{-3/2}(\eta_\mathrm{q})J_{-1/2}^{-2}(\eta_\mathrm{q}). \tag{A.7}$$

The Skyrme parameters of the SkM* force are

$$\begin{aligned} & t_0 = -2645\ \mathrm{MeV}\cdot\mathrm{fm}^3, && x_0 = 0.09, \\ & t_1 = 410\ \mathrm{MeV}\cdot\mathrm{fm}^5, && W_0 = 130\ \mathrm{MeV}\cdot\mathrm{fm}^5, \\ & t_2 = -135\ \mathrm{MeV}\cdot\mathrm{fm}^5, && \alpha = \tfrac{1}{6}. \\ & t_3 = 15\,595\ \mathrm{MeV}\cdot\mathrm{fm}^{3+3\alpha}, \end{aligned} \tag{A.8}$$

We frequently use the following combinations of the Skyrme parameters

$$\begin{aligned} & c_0 = \tfrac{1}{8}(3t_1-t_2), && c_4 = (1+\tfrac{1}{2}x_0)t_0, && c_8 = \tfrac{1}{4}(1-x_0)t_0, \\ & c_1 = \tfrac{3}{16}(t_1-t_2), && c_5 = (\tfrac{1}{2}+x_0)t_0, && c_9 = \tfrac{1}{8}(3t_1+5t_2), \\ & c_2 = \tfrac{1}{4}(t_1+t_2), && c_6 = \tfrac{1}{12}t_3, && c_{10} = \tfrac{1}{16}(9t_1-5t_2). \\ & c_3 = \tfrac{1}{8}(t_2-t_1), && c_7 = \tfrac{1}{8}(t_1+3t_2), \end{aligned} \tag{A.9}$$

Appendix B

FUNCTIONS OCCURRING IN THE DIFFERENTIAL EQUATION

The differential equation in spherical symmetry reads

$$\rho_q''(r) = \frac{c_q[\beta_{\bar{q}}(r) + V_q(r)] + B_{\bar{q}}(r)[\beta_q(r) + V_q(r)]}{c_q^2 - B_q(r)B_{\bar{q}}(r)} \tag{B.1}$$

introducing the definitions

$$B_q(r) = c_1 - 2\beta_w h_q \xi_q / \rho_q \,, \tag{B.2}$$

$$\beta_q(r) = \tilde{\beta}_q(r) - \frac{2}{r} c_1 \rho_q' - \frac{2}{r} c_0 \rho_{\bar{q}}' - h_q 4\beta_W \xi_q \rho_q' / \rho_q \,, \tag{B.3}$$

with

$$\tilde{\beta}_q(r) = T\eta_q + e_q(r) + f_q(r) - \lambda_q + J_{3/2}(\eta_q) T A_q h_q^{-1} c_7 + J_{3/2}(\eta_{\bar{q}}) T A_{\bar{q}} h_q^{-1} c_2 \,, \tag{B.4}$$

$$e_q(r) = 2c_8\rho_q + \tfrac{1}{2}c_4\rho_q + c_6(\rho_q + \rho_q)^{\alpha+1}(\alpha+2)/2 \,, \tag{B.5}$$

$$\begin{aligned} f_q(r) = {} & \beta_w(c_7\xi_q\rho_q'^2/\rho_q + c_2\xi_{\bar{q}}\rho_{\bar{q}}'^2/\rho_{\bar{q}} + (\partial\xi_{\bar{q}}/\partial\eta_{\bar{q}}\partial\eta_{\bar{q}}/\partial\rho_q\rho_{\bar{q}}'^2)h_{\bar{q}}/\rho_{\bar{q}} \\ & + (-\partial\xi_q/\partial\eta_q\partial\eta_q/\partial\rho_q\rho_q'^2 + \xi_q\rho_q'^2/\rho_q - 2\partial\xi_q/\partial\eta_q\partial\eta_q/\partial\rho_{\bar{q}}\rho_q'\rho_{\bar{q}}')h_q/\rho_q) \,. \end{aligned} \tag{B.6}$$

The derivatives in eq. (B.6) can be evaluated in terms of the generalized Fermi integrals as

$$\partial\xi_q/\partial\eta_q = \frac{-J_{-3/2}(\eta_q)}{24J_{-1/2}(\eta_q)} + \frac{J_{1/2}(\eta_q)J_{-5/2}^2(\eta_q)}{8J_{-1/2}^2(\eta_q)} - \frac{J_{1/2}(\eta_q)J_{-3/2}^2(\eta_q)}{12J_{-1/2}^3(\eta_q)} \,. \tag{B.7}$$

$$\partial\eta_q/\partial\rho_q = \frac{2 + 3h_q^{-1}c_7\rho_q}{A_q J_{-1/2}(\eta_q)} \,, \tag{B.8}$$

$$\partial\eta_{\bar{q}}/\partial\rho_{\bar{q}} = \frac{3c_2 J_{1/2}(\eta_q)}{h_q J_{1/2}(\eta_{\bar{q}})} \,. \tag{B.9}$$

The Coulomb potential in spherical symmetry is

$$V_p(r) = 4\pi e^2 \left(\frac{1}{r}\int_0^r \mathrm{d}r'\, r'^2 \rho_p(r') + \int_r^R \mathrm{d}r'\, r'\rho_p(r') \right) . \tag{B.10}$$

Appendix C

LIMITS OF THE DIFFERENTIAL EQUATION

C.1. The limit $r \to 0$. The problematic terms in the differential eqs. (2.16) are those containing $1/r$. We first note that the boundary condition at $r = 0$ is $\rho_q'(r=0) = 0$ (no kink at the center of the nucleus). Using this, a Taylor expansion of ρ_q' around

$r=0$ yields $\lim_{r\to 0}(\rho_q'/r)=\rho_q''$. This substitution redefines c_q, β_q and B_q in the differential equations as

$$c_q \to 3c_q\,, \qquad B_q \to 3B_q\,, \qquad \beta_q \to \tilde{\beta}_q\,. \tag{C.1}$$

Taking the limit $r\to 0$ of the Coulomb energy term leads to the substitution

$$a_p \to 4\pi e^2 \int_0^R \mathrm{d}r'\, r'\rho_p(r')\,. \tag{C.2}$$

C.2. Vanishing denominator in the differential equation. The last step in the derivation of the differential eq. (2.16) was to divide the equation

$$(c_q^2 - B_q B_{\bar{q}})\rho_q'' = c_q(\beta_{\bar{q}} + V_{\bar{q}}) + \beta_{\bar{q}}(\beta_q + V_q) \tag{C.3}$$

by the factor in front of ρ_q''. This factor vanishes in the limit $c_q^2 \to B_{\bar{q}}B_q$ or

$$B_{\bar{q}} = c_q^2/B_q\,. \tag{C.4}$$

Requiring ρ'' to stay finite, the r.h.s. of (C.3) becomes zero, yielding

$$B_{\bar{q}} = -c_q(\beta_{\bar{q}} + V_{\bar{q}})/(\beta_q + V_q)\,. \tag{C.5}$$

Inserting (C.4) into the r.h.s. of (C.3) and using (C.5), one obtains $(c_q^2 - B_q B_{\bar{q}})\rho_q'' = (\beta_q + V_q)(c_q^2 - B_q B_{\bar{q}})/B_q$ which results in the limit

$$\rho_q'' \to (\beta_q + V_q)/B_q \qquad \text{if} \quad c_q^2 - B_q B_{\bar{q}} \to 0\,. \tag{C.6}$$

Appendix D

CORRECTION TERMS

In this appendix, we consider correction terms due to the spin-orbit energy and the gradients of the effective mass.

(i) The Skyrme spin-orbit free-energy density is

$$\mathcal{F}_{\mathrm{s.o.}} = -\tfrac{1}{8}W_0^2 \sum_{q=n,p} h_q^{-1}\rho_q(2\nabla\rho_q + \nabla\rho_{\bar{q}})^2\,. \tag{D.1}$$

(ii) Taking proper care of the gradients of h_q leads to an extra term $\mathcal{F}^*$ in the free-energy density,

$$\mathcal{F}^* = \sum_{q=n,p} [(\tfrac{9}{4}\xi_q - \tfrac{7}{48})\rho_q h_q^{-1}(\nabla h_q)^2 + (3\xi_q - \tfrac{5}{12})\nabla\rho_q\nabla h_q] \tag{D.2}$$

since the kinetic-energy density (A.2) has now additional terms

$$\mathcal{E}_{\mathrm{kin}}^* = \sum_{q=n,p} [h_q^{-1}(\nabla h_q)^2\rho_q(\tfrac{9}{4}\mathcal{C}_q - \tfrac{7}{48}) + \nabla h_q\nabla\rho_q(3\mathcal{C}_q - \tfrac{5}{12}) + \tfrac{1}{3}\nabla h_q\nabla\rho_q]\,. \tag{D.3}$$

and the full entropy including gradients of the effective mass is

$$\sigma = \sum_{q=n,p}\left[\tfrac{5}{3}A_q J_{3/2}(\eta_q) - \eta_q\rho_q - \frac{\nu_q}{T}\left(h_q W\frac{(\nabla\rho_q)^2}{\rho_q} + \tfrac{9}{4}\nabla h_q h_q^{-1}\rho_q + 3\nabla h_q\nabla\rho_q\right)\right] \tag{D.4}$$

with

$$\nu_q = -\tfrac{3}{2}\xi_q + 36\xi_q^2 - \omega_q \,. \tag{D.5}$$

(iii) In performing the variation (2.3), extra terms arise in $\delta\mathscr{F}_2/\delta\rho_q$ if ∇h_q is taken into account. This can be expressed simply by the substitution

$$\frac{\delta\mathscr{F}_2}{\delta\rho_q} \to \frac{\delta\mathscr{F}_2}{\delta\rho_q} - \nabla h_q \xi_q \frac{2\nabla\rho_q}{\rho_q} \,. \tag{D.6}$$

Adding the contributions from (i), (ii) and (iii) in the derivation of the differential equation in spherical symmetry, we arrive at a differential equation like eq. (2.15), where the changes to be made are the substitutions

$$B_q \to B_q + d_1 + W_0^2(h_q{}^{-1}\rho_q + \tfrac{1}{4}h_{\bar q}{}^{-1}\rho_{\bar q}) \tag{D.7}$$

$$c_q \to c_q - d_2 - W_0^2(\tfrac{1}{2}h_q^{-1}\rho_q + \tfrac{1}{2}h_{\bar q}^{-1}\rho_{\bar q}) \tag{D.8}$$

$$\tilde\beta_q \to \tilde\beta_q + s_q + m_q - \nabla h_q \tag{D.9}$$

now with

$$\beta_q = \tilde\beta_q - \frac{2c_1}{r}\rho_q' - \frac{2c_0}{r}\rho_{\bar q} - h_q\frac{4}{\rho_q r}W\xi_q\rho_q' + \frac{2}{r}d_1\rho_q' + \frac{2}{r}d_2\rho_{\bar q}'$$
$$+\frac{2}{r}W_0^2\rho_q'(h_q^{-1}\rho_q + \tfrac{1}{4}h_{\bar q}^{-1}\rho_{\bar q}) + \frac{2}{r}W_0^2\rho_{\bar q}'(\tfrac{1}{2}h_q^{-1}\rho_q + \tfrac{1}{2}h_{\bar q}^{-1}\rho_{\bar q}) \,. \tag{D.10}$$

The new functions introduced in the equations above are

$$d_1 = -(\tfrac{9}{4}\xi_q - \tfrac{7}{48})h_q^{-1}2c_7^2\rho_q - (\tfrac{9}{4}\xi_{\bar q} - \tfrac{7}{48})h_{\bar q}^{-1}2c_2^2\rho_{\bar q} - 6c_7\xi_q + \tfrac{5}{6}c_7 \tag{D.11}$$

$$d_2 = -(\tfrac{9}{4}\xi_q - \tfrac{7}{48})h_q^{-1}2c_2c_7\rho_q - (\tfrac{9}{4}\xi_{\bar q} - \tfrac{7}{48})h_{\bar q}^{-1}2c_2c_7\rho_{\bar q} - 3c_2(\xi_q + \xi_{\bar q}) + \tfrac{5}{6}c_2 \tag{D.12}$$

$$s_q = -\tfrac{1}{8}W_0^2h_q^{-2}(2\rho_q' + \rho_{\bar q}')[(2\rho_q' + \rho_{\bar q}')(h_q - c_7\rho_q) + 4\rho_q h_q' - 4h_q\rho_q']$$
$$-\tfrac{1}{8}W_0^2h_{\bar q}^{-2}(2\rho_{\bar q}' + \rho_q')[(2\rho_{\bar q}' + \rho_q')(h_{\bar q} - c_2\rho_{\bar q}) - 2\rho_{\bar q}h_{\bar q}' - 2h_{\bar q}\rho_{\bar q}'] \tag{D.13}$$

$$m_q = \left(\frac{9}{4}\frac{\partial\xi_q}{\partial\eta_q}\frac{\partial\eta_q}{\partial\rho_q}h_q^{-1}\rho_q + (\tfrac{9}{4}\xi_q - \tfrac{7}{48})h_q^{-1}\right)(c_2^2(\nabla\rho_{\bar q})^2 - c_7^2(\nabla\rho_q)^2)$$
$$+(\tfrac{9}{4}\xi_q - \tfrac{7}{48})h_q^{-2}\rho_q c_7(c_7\nabla\rho_q + c_2\nabla\rho_{\bar q})^2$$
$$+\frac{9}{4}\frac{\partial\xi_q}{\partial\eta_{\bar q}}\frac{\partial\eta_{\bar q}}{\partial\rho_q}\rho_{\bar q}h_{\bar q}^{-1}(c_7^2(\nabla\rho_{\bar q})^2 - c_2^2(\nabla\rho_q)^2) + (\tfrac{9}{4}\xi_{\bar q} - \tfrac{7}{48})\rho_{\bar q}h_{\bar q}^{-2}c_2(c_7\nabla\rho_{\bar q} + c_2\nabla\rho_q)^2$$
$$+3\frac{\partial\xi_{\bar q}}{\partial\eta_{\bar q}}\frac{\partial\eta_{\bar q}}{\partial\rho_q}(\nabla\rho_{\bar q})^2c_7 - \frac{\partial\xi_q}{\partial\eta_q}\frac{\partial\eta_q}{\partial\rho_{\bar q}}\nabla\rho_{\bar q}(c_7\nabla\rho_q + c_2\nabla\rho_{\bar q})(\tfrac{9}{2}\rho_q h_q^{-1}c_7 + 3)$$
$$-\frac{\partial\xi_{\bar q}}{\partial\eta_{\bar q}}\frac{\partial\eta_{\bar q}}{\partial\rho_{\bar q}}\nabla\rho_{\bar q}c_2((c_7\nabla\rho_{\bar q} + c_2\nabla\rho_q)\tfrac{9}{2}\rho_{\bar q}h_{\bar q}^{-1} + 3\nabla\rho_{\bar q})$$
$$-(\tfrac{9}{4}\xi_{\bar q} - \tfrac{7}{48})(c_7\nabla\rho_{\bar q} + c_2\nabla\rho_q)2c_2h_{\bar q}^{-1}\nabla\rho_{\bar q}$$
$$-3\frac{\partial\xi_q}{\partial\eta_q}\left(\frac{\partial\eta_q}{\partial\rho_q}\nabla\rho_q + \frac{\partial\eta_q}{\partial\rho_{\bar q}}\nabla\rho_{\bar q}\right)\nabla\rho_q c_7 \,. \tag{D.14}$$

References

1) J.E. Finn *et al.*, Phys. Rev. Lett. **49** (1982) 1321;
R.W. Minich *et al.*, Phys. Lett. **B118** (1982) 458;
A.S. Hirsch *et al.*, Phys. Rev. **C29** (1984) 508;
N.T. Porile *et al.*, Phys. Lett. **B156** (1985) 177
2) P. Bonche, S. Levit and D. Vautherin, Nucl. Phys. **A427** (1984) 278
3) P. Bonche, S. Levit and D. Vautherin, Nucl. Phys. **A436** (1985) 265
4) E. Suraud and D. Vautherin, Phys. Lett. **B138** (1984) 325;
E. Suraud, Nucl. Phys. **A462** (1987) 109
5) A.H. Blin, B. Hiller, H. Reinhardt and P. Schuck, J. de Phys. **47** (1986) C4-423;
A.H. Blin, M. Brack and B. Hiller, Phys. Lett. **B182** (1986) 239;
A.H. Blin, B. Hiller, H. Reinhardt and P. Schuck, Nucl. Phys. **A484** (1988) 295
6) M. Brack, Phase space approaches to nuclear dynamics, ed. M. di Toro *et al.* (World Scientific, Singapore, 1986) p. 417;
M. Brack, Windsurfing the fermi sea, ed. T.T.S. Kuo and J. Speth, vol. II (North-Holland, Amsterdam, 1987) p. 219
7) H.N.V. Temperley, Proc. Phys. Soc. **59** (1947) 199
8) W. Stocker and J. Burzlaff, Nucl. Phys. **A202** (1973) 265
9) P. Siemens, Nature **305** (1983) 410; Nucl. Phys. **A428** (1984) 197c
10) M. Brack, C. Guet and H.-B. Håkansson, Phys. Report, **123** (1985) 275;
J. Bartel, M. Brack and M. Durand, Nucl. Phys. **A445** (1985) 263
11) O. Bohigas, A.M. Lane and J. Martorell, Phys. Reports **51** (1979) 267
12) P. Gleissl, M. Brack, J. Meyer and P. Quentin, Ann. of Phys. (1989) in press; and private communication
13) D.D. Clayton, Principles of stellar evolution and nucleosynthesis (McGraw-Hill, New York, 1968)
14) J.M. Blatt and V.F. Weisskopf, Theoretical nuclear physics (Springer, New York, 1979)
15) M. Brack, Density functional methods in physics, ed. R. Dreizler and J. da Providencia (Plenum, New York 1985) p. 331
16) W. Stocker, P. Gleissl and M. Brack, Nucl. Phys. **A471** (1987) 501;
P. Gleissl, private communication
17) C. Guet, E. Strumberger and M. Brack, Phys. Lett. **B205** (1988) 427
18) See various contributions to 'HICOFED'. Int. Conf. on heavy ion nuclear collisions in the fermi energy domain, Caen 1986, J. de Phys. **C4** (1986)